ISSN 2176-5480

22nd International Congress of Mechanical Engineering (COBEM 2013)
November 3-7, 2013, Ribeirão Preto, SP, Brazil

HIGH CYCLE FATIGUE BEHAVIOR OF THREE Al-Mg-Si ALLOYS

Ana Márcia Barbosa da Silva
Escola de Engenharia de Lorena, Universidade de São Paulo – EEL/USP, Departamento de Engenharia de Materiais - DEMAR, Pólo Urbo Industrial-Gleba Al6-Bairro Mondesir Lorena – Lorena/SP, Brazil
anamarcia2359@gmail.com

Carlos Antonio Reis Pereira Baptista
Escola de Engenharia de Lorena, Universidade de São Paulo – EEL/USP, Departamento de Engenharia de Materiais - DEMAR, Pólo Urbo Industrial-Gleba Al6-Bairro Mondesir Lorena – Lorena/SP, Brazil
baptista@demar.eel.usp.br

Marcelo Augusto Santos Torres
Universidade Estadual Paulista "Júlio de Mesquita Filho" – UNESP, Departamento de Mecânica - DME, Av. Ariberto Pereira da Cunha, 333-Bairro Pedregulho – Guaratinguetá/SP, Brazil
mastorres@uol.com.br

Anderson Gandra Kuster
Universidade Estadual Paulista "Júlio de Mesquita Filho" – UNESP, Departamento de Mecânica - DME, Av. Ariberto Pereira da Cunha, 333-Bairro Pedregulho – Guaratinguetá/SP, Brazil
gandra149@gmail.com

Abstract. *Aluminum alloys have been widely used in mobile structures such as land vehicles and aircraft due to their favorable strength-to-weight ratio. Among these alloys, the automotive industry has shown a growing interest in the 6xxx (Al-Mg-Si) series due to their good mechanical strength, easy fabrication and excellent corrosion resistance. Studies of the fatigue behavior are always a need, also in the automotive industry, because the structural components are subjected to vibratory loads and cyclic stresses and, as a consequence, may eventually crack and fracture. In this study, fatigue tests were performed in three Al-Mg-Si alloys, namely AA 6005, AA 6351 and AA 6063, tempered and aged for the T6 condition. The fatigue tests were conducted in a rotating bending machine (R = -1) at a frequency of 40 Hz and at room temperature. Two distinct surface finishes were adopted for the specimens: as-machined and polished. The notch sensitivity was also assessed by testing V-notch specimens (K_t = 3.0). The fatigue test results in all conditions were analyzed using the Maximum-Likelihood method. The results allowed to determine the differences in fatigue behavior of the three alloys. Micrographic and fractographic analyses were performed in order to support discussions on the fatigue results.*

Keywords: *aluminum alloys, high cycle fatigue, surface finishing, notch sensitivity, stress concentration, Maximum-Likelihood method*

1. INTRODUCTION

The 6xxx series are medium strength structural aluminum alloys, with good weldability, good corrosion resistance and high damping capacity. These alloys represent a high volumetric fraction of extruded aluminum alloys which are produced for commercial use and have been increasingly applied in the automotive industry due to its high ratio strength / weight (Azzam, et al., 2010; Burger, et al. 1995; Cayron and Buffat, 2000; Polmear, 1995). The Companhia Brasileira de Alumínio (CBA) started the production of these three alloys, in T6 condition which are solubilized and then artificially aged at a temperature of 180ºC for 6 hours. Therefore, the mechanical properties of these materials, particularly their fatigue resistance, need to be better understood. This study adds to other research to better analyze the performance of AA 6005, AA 6063, AA 6351 alloy for automotive industry application (Espezua, et al., 2012; Laurito, et al., 2012; Silva, 2012; Silva, et. al., 2012).

The fatigue is a continuous degradation of a component submitted to cyclic loading, which may lead to rupture of the material due to the nucleation and further propagation of one or multiple cracks. Fatigue fractures are caused by the simultaneous action of cyclic stress, tensile stress and plastic deformation. The absence of one of these three factors prevents the occurrence of the phenomenon (Baptista, 2000). The cyclic stress initiates the fatigue crack, the tensile stress causes the propagation; irreversible nature of plastic yielding contributes to the accumulation of damage in each cycle (Sadananda and Ramaswamy, 2001).

The preferred site for the nucleation of a fatigue crack is the free surface of a structure or a component. Thus, the preparation of the surface during manufacturing of the structure or component has important influence in the initiation life for fatigue cracks. Moreover, machining operations such as polishing and milling, result in different degrees of surface roughness. The irregularities on the rough surface act as stress concentration, which, in turn, causes the variation

ISSN 2176-5480

of resistance to fatigue crack nucleation. The notches can act as crack nucleation sites and thus decrease the fatigue life; Since this topic is of considerable interest for a wide variety of engineering applications (Suresh, 1998), notch effect in fatigue resistance varies substantially, depending on the material and the geometry of the notch (Mcevily et al., 2008).

In this study, fatigue tests were performed in the AA 6005, AA 6351 and AA 6063 aluminum alloys, tempered and aged for the T6 condition. The fatigue tests were conducted in a rotating bending machine (R = -1) at a frequency of 40 Hz and at room temperature. Two distinct surface finishes were adopted for the specimens: as machined and polished. The notch sensitivity was also assessed by testing V-notch specimens (K_t = 3.0). The fatigue test results in all the conditions were analyzed using the Maximum-Likelihood method. In order to support the discussions on fatigue, EDS analyses (Energy Dispersive Spectrography) were performed to determine the composition of the second phase particles, and also fractographic analysis with a scanning electron microscope in order to study the points of cracks initiation.

2. MATERIALS AND METHODS

This research was conducted using Al-Mg-Si aluminum alloys (AA 6005, AA 6351 and AA 6063) with a T6 heat treatment (solubilized at 580°C and artificially aged at 180°C - 6 hours). The alloy's chemical compositions and the mechanical properties are shown in Tab. 1 and Tab. 2, in which σ_e is the yield stress, σ_t is the ultimate tensile strength, ε represents the percent elongation and E the Young's Modulus.

Table 1. Chemical composition of the Al-Mg-Si T6 aluminum alloys (weight %).

Alloy	Si	Fe	Cu	Mn	Mg	Cr	Zn	Ti
AA 6005	0.50 - 0.9	0.35	0.30	0.50	0.40 - 0.7	0.30	0.20	0.10
AA 6351	0.7 - 1.3	0.5	0.10	0.40 - 0.8	0.40 - 0.8	-	0.20	0.20
AA 6063	0.2 - 0.6	0.35	0.10	0.10	0.45 - 0.9	0.10	0.10	0.10

Table 2. Mechanical properties of the Al-Mg-Si T6 alloys.

	6005	6351	6063
σ_T (MPa)	286	353	261
σe (MPa)	256	330	229
ε (%)	18	15	18
E (GPa)	65	67	63

The sectioned samples of the Al-Mg-Si were metallographically prepared with methods of standard surface preparation. The specimens were etched with hydrofluoric acid 0.5% and observed in the optical Microscope Olympus BX51M. Fracture surfaces were analyzed by Scanning Electron Microscopy (SEM) and Energy Dispersive Spectrography (EDS) using a microscope LEO mod. 1450VP. The high cycle fatigue tests were performed in the Fatigue Dynamics Machine – RBF 200 model (Fig. 1) in rotary bending fatigue conditions (R = -1). The frequency used was 40 Hertz at room temperature. The fatigue tests were performed in accordance with the ASTM E739-10 standard that determines the minimum number of 6 to 12 tests and replication over 50% for research and development level (ASTM, 2010). The fatigue machine was adjusted so that the specimens suffered minimum vibration during the test, ensuring that the test conditions remained constant and did not affect the scattering of the fatigue results.

Figure 1 - Fatigue Dynamics Machine model RBF 200.

ISSN 2176-5480

The specimen dimensions used in the fatigue tests are indicated in Fig.2 (a) polished/as-machined and (b) notched. The radius of the 0.1mm depth notch was verified by using the Projector Profiling Pantec DP-100 model, with 100x lens.

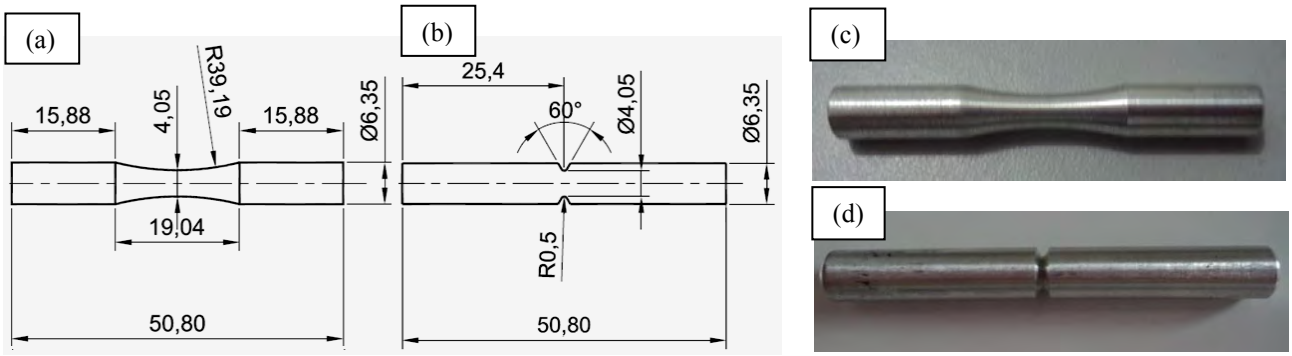

Figure 2. Dimensions of specimens used in the high cycle fatigue tests (a, c) polished/ as-machined and (b, d) notched.

3. RESULTS AND DISCUSSIONS

3.1. Microstructural Analysis

In Figure 3 (a), (b) and (c) the micrographs of the AA 6005, AA 6351 and AA 6063 alloys are shown. Among the analyzed materials, the AA 6005 and AA 6351 alloys present second phase particles with rounded shapes and maximum size of 3 and 5 μm, respectively and it is constituted by α-(Fe, Mn)SiAl phase. The AA 6063 alloy presents elongated particles of the α-FeSiAl phase with maximum size of 8 μm.

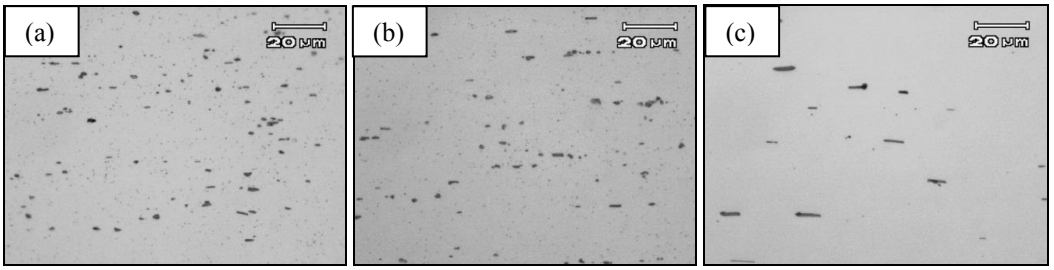

Figure 3 - Micrographs of the (a) AA 6005, (b) AA 6351 and (c) AA 6063 alloys – 500X.

Figure 4 shows a micrograph of the AA 6351 alloy where it is possible to observe the grain boundary and the presence of the intermetallic second phase (white points).

Figure 4 - Micrograph of the (a) AA 6351 alloys (Silva, 2012)

ISSN 2176-5480

Table 3 presents the volumetric fraction of the second phase particles, which was calculated using the software IMAGE J 1.30. It can be observed that AA 6005 presents the higher volumetric fraction of the second phase particles.

Table 3. The volumetric fraction of the second phase particles.

Alloy	**Volumetric fraction of the second phase particles (%)**	**Standard deviation (SD)**
AA 6005	3.0	± 0.3
AA 6351	2.7	± 0.2
AA 6063	2.5	± 0.2

By means of EDS analysis it was observed that second phase particles in the AA 6063 alloy are mainly constituted by Al, Fe and Si. Furthemore, in most analyses Mn and Cr were not detected or found in very low amounts.

In these conditions it is quite probable that the particles are constituted by the Fe_3SiAl_{12}, $Fe_2Si_2Al_9$ phases or by their combination, depending on the proportion of the Mg, Si and Fe. These are the phases rich in Fe (most common impurity found in aluminum) when Mn and Cr are not present (Hatch, 1984).

On the other hand, the EDS analyses of the AA 6351 and AA 6005 alloys show that second phase particles are mainly constituted by Al, Fe, Si and Mn. Therefore, these particles should be constituted mainly of $(Fe, Mn, Cr)_3SiAl_{12}$ phase; however, it is interesting to highlight that the AA 6351 alloy does not present Cr in its composition.

3.2 Fatigue tests

The Figure 5 (a), (b) and (c) presents the fatigue results for the polished condition (specimens shown in Fig. 2 (a)) for the AA 6005, AA 6351 and AA 6063 alloys, respectively.

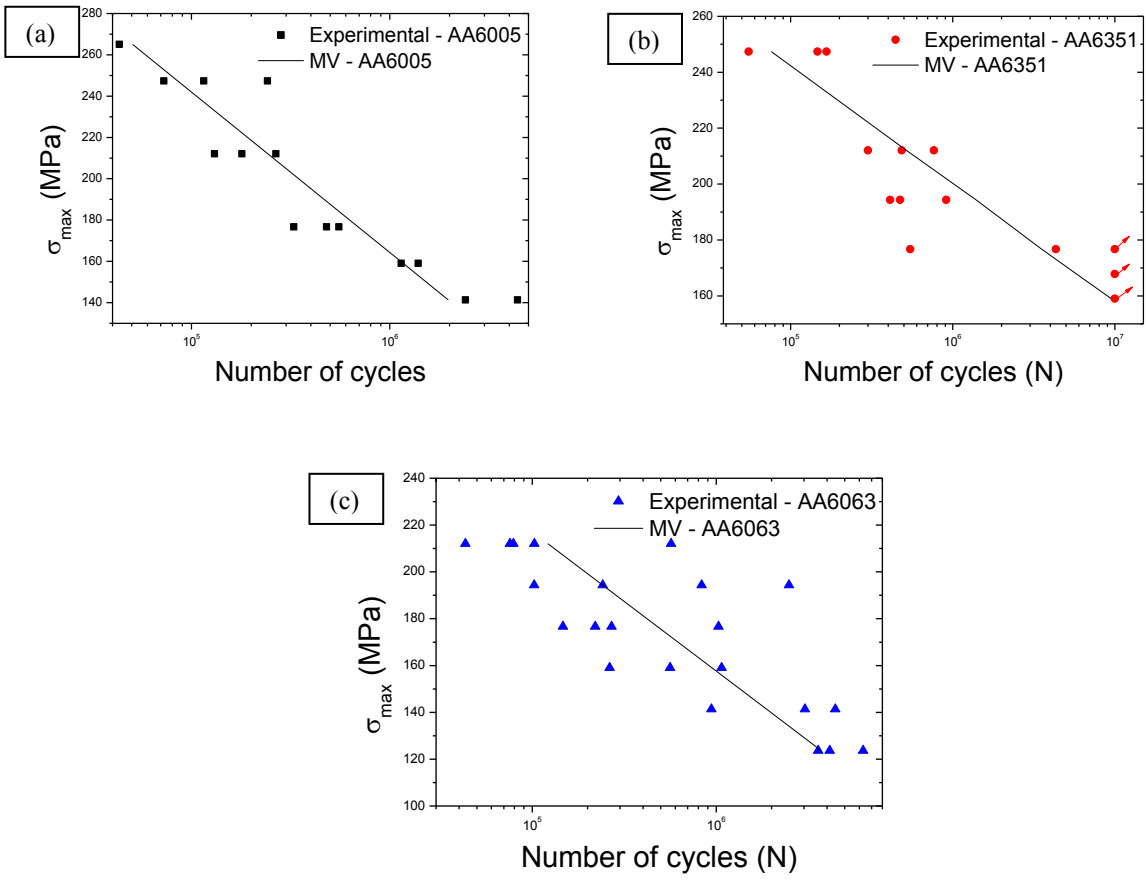

Figure 5. Model fitting using the Maximum-Likelihood Method: (a) AA 6005 alloy; (b) AA 6351 alloy; (c) AA 6063 (polished condition).

ISSN 2176-5480

In Figure 6 the overlap of the fatigue results of the polished condition of the specimens (Fig. 2 (a)) is presented. The experimental data were fitted to the Log-Linear model by using the Maximum Likelihood Method and the resulting equations are shown in Tab. 4. This method presents a solid approach for problems of parameter estimation besides being able to incorporate runouts in the analysis of the S/N curves.

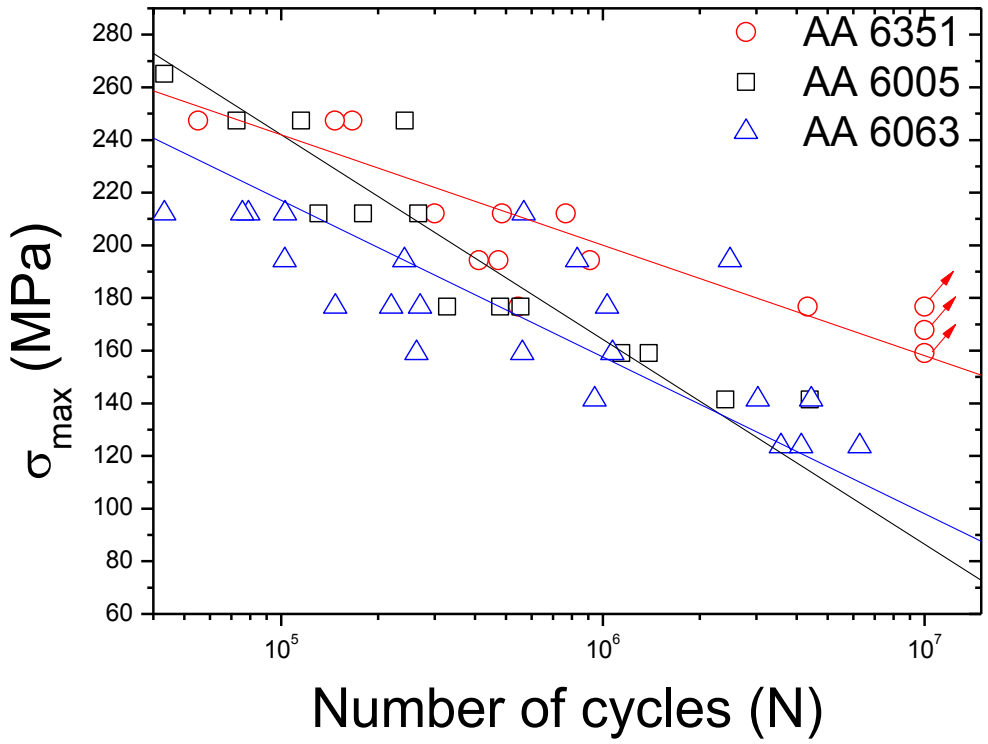

Figure 6. Model fitting using the Maximum-Likelihood Method: AA 6005, AA 6351 and AA 6063 (polished condition).

Table 4. Equations obtained by the Maximum Likelihood Method-polished condition.

Alloy	**Equation**
AA 6005	log N = 8.11298 - 0.0128657 *(σ_{max})
AA 6351	log N = 10.7674 - 0.0238341 *(σ_{max})
AA 6063	log N = 8.64937 - 0.0168160 *(σ_{max})

In Figure 6 it was observed that the AA 6351 alloy tends to a fatigue limit of 180 MPa (first runout) and the AA 6005 and AA 6063 showed failure of specimens below of this stress. A lower scattering of AA 6005 can also be observed, indicated by the standard deviation (SD=0.2208), when compared to the AA 6351 alloy (SD=0.3831) and mainly when compared to AA 6063 alloy (SD = 0.4125). The comparison of S/N curves for the three alloys studied in the polished condition (Fig.6) shows that the AA 6351 alloy presents better fatigue behavior than the AA 6005 and AA 6063. Regarding the AA 6005 and AA 6063 alloys, the Maximum Likelihood Method suggests an improvement in fatigue behavior of the AA 6005 alloy when compared to the AA 6063 alloy, mainly for low and medium cycle.

The Figures 7 (a), (b), (c) and (d) show the fatigue results those specimens which were as-machined (Fig. 2 (a)). For the treatment of experimental data it was also used the Maximum Likelihood Method whose equations are presented in Table 5. As for the as-machined condition, the three alloys showed a tendency to present a fatigue limit between 140 MPa and 150 MPa. The AA 6005 alloy (SD=0.1681) showed again lower scattering when compared to AA 6351 (SD=0.2557) and AA 6063 (SD=0.2630) alloys. The scattering observed in the fatigue results are not due to misalignment of the equipment or deficient techniques applied, but it is directly related to the material characteristic factors, such as inclusions or grain size differences. Thus, for the fatigue is customary to work with the average life and the standard deviation within acceptable confidence limits (Fonseca Jr., 2003). In this context, the scattering in samples

ISSN 2176-5480

is partially associated with changes in the crack nucleation sites (in surface imperfections or in the second phase particles present in the material, for example) (ASM, 1996). It can also be observed that in both conditions (polished and as machined), the increase in scattering is proportional to the increase in the size the second phase particles present in the alloys (item 3.1). The fatigue behavior of the materials is highly sensitive to many variables such as surface of specimen effects and metallurgical variables. In these alloys, the fatigue crack growth can be highly influenced by the particles content as well as by the type of age hardening heat treatment (Borrego, et. al., 2004).

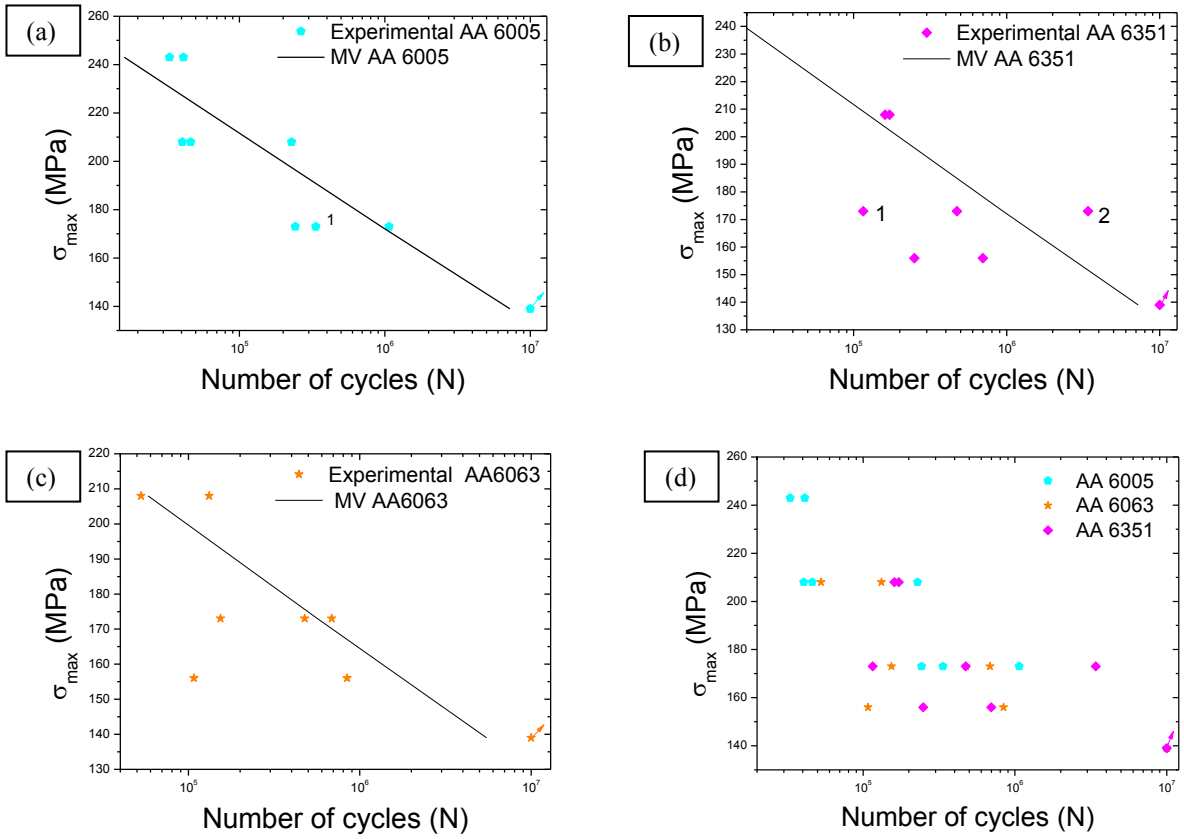

Figure 7. Model fitting using the Maximum-Likelihood Method: (a) AA 6005 alloy; (b) AA 6063 alloy; (c) AA 6351 and (d) all the experimental results as machined condition.

Table 5. Equations obtained by the Maximum Likelihood Method - as machined condition

Alloy	**Equation**
AA 6005	$\log N = 10.3941 - 0.0255113*(\sigma_{max})$
AA 6351	$\log N = 9.32366 - 0.0204461*(\sigma_{max})$
AA 6063	$\log N = 9.71449 - 0.0237819*(\sigma_{max})$

Regarding the surface effect, the roughness of the specimen and surface damage produced during machining (grooves, scratches, burrs, etc.) in the preparation of the specimens can be highlighted. The Tab. 6 shows the values of average roughness of the specimens in the polished condition, whose fatigue curves were shown in Fig.6 and the average roughness of the specimens as machined, whose fatigue curves are shown in Fig. 7 (d).

ISSN 2176-5480

Table 6. Surface roughness of the specimens.

Type of roughness	AA 6005		AA 6063		AA 6351	
	as machined	polished	as machined	polished	as machined	polished
Ra	3.36	0.45	2.81	0.47	3.24	0.36
Ry	13.95	2.7	10.8	2.9	12.43	2.67

In Table 6 it can be observed that the surface roughness (Ra) of the as machined specimens without polishing was at least 5 times higher than the surface roughness of the polished specimens.

Considering that the tests were performed in bending fatigue conditions, the highest stresses occurred on the surface of the specimens. A higher level of stress on the surface, combined with surface roughness, cause the fatigue crack initiation, mainly on the surface of the specimens. Figure 8 shows the fracture surface of a specimen fractured of AA 6351 alloy (Point 1 of Fig. 7 (b)). It can be observed that there are many sites of crack initiation on the surface (marked with arrows), all of them contributing to the fracture.

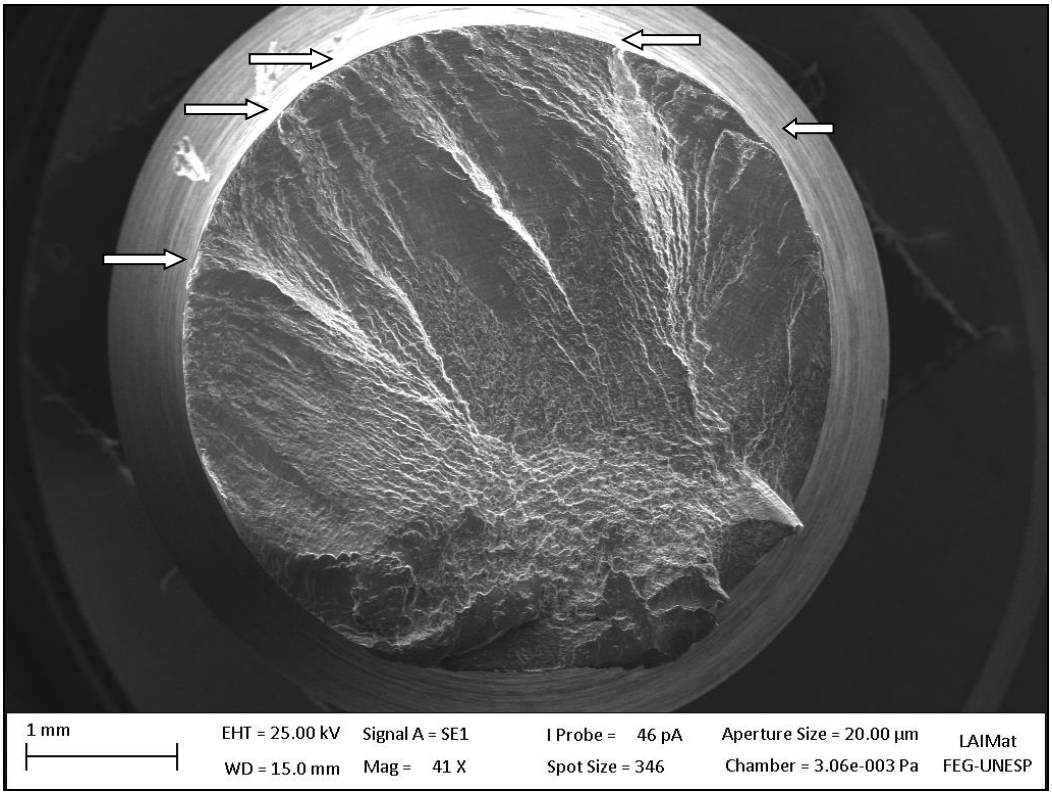

Figure 8. Fractography of the AA 6351 alloy tested at 173 MPa and fractured after 115,400 loading cycles.

In Figure 9 it can be observed the fracture surface under the stress of 173 MPa (Point 2 of Fig. 7 (b)). It is observed that the specimens shown in Figures 8 and 9 belong to the same alloy, but showed the biggest difference in the number of cycles to fracture of all tests performed for the same stress.

It can be seen in Fig. 9 that the crack initiation occurred essentially at one point (indicated by arrow), showing a different behavior found in the Fig. 8. Therefore, it can be considered that a higher amount of surface defects creates a larger number of sites of crack nucleation and may lead to shorter fatigue life.

ISSN 2176-5480

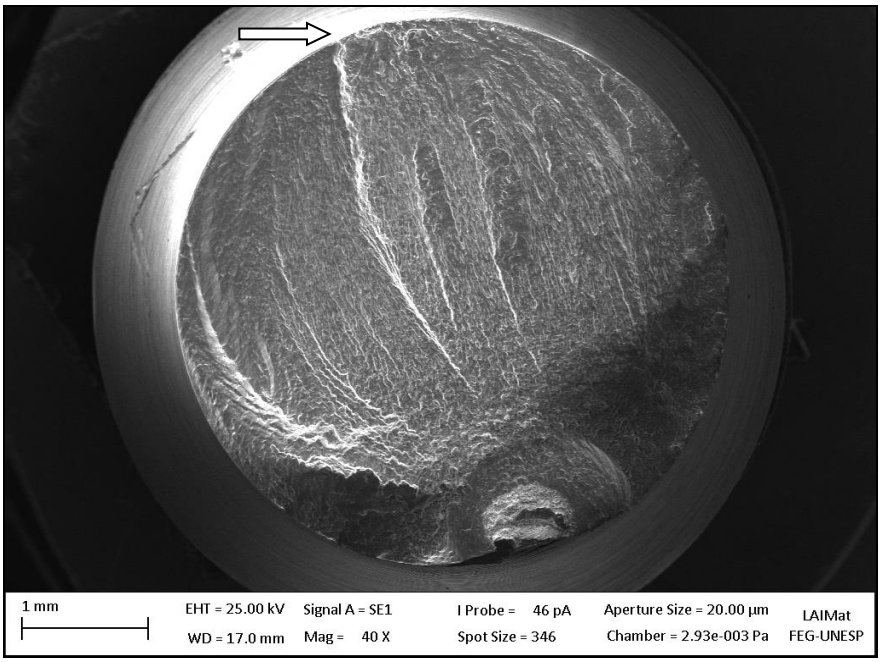

Figure 9. Fractography of the AA 6351 alloy tested at 173 MPa and fractured after 3,405.900 loading cycles.

The metallurgical variables such as grain size and the presence of second phase particles also have an important influence in material fatigue resistance. Several studies have been conducted in AlMgSi aluminum alloys, that demonstrate the greater influence of the second phase particles (Borrego, et al., 2004; Christ and Mughrabi, 1996). The coarse particles in aluminum alloys act as stress concentrators, serving as nucleation sites for fatigue crack. In Fig. 3 it can be observed the presence of second phase particles in the micrograph of AA 6351 alloy. The scattering of the results can also be associated with the existence of large amounts of second phase particles. This behavior creates certain heterogeneity in material and also induces stress concentrators on the surface or inside the specimen influencing the crack initiation and the rate of the crack propagation. The Fig. 10 shows a crack initiation site from a second phase particle, close to the surface (marked with arrow) in the specimen number 1 in Fig. 5. (a).

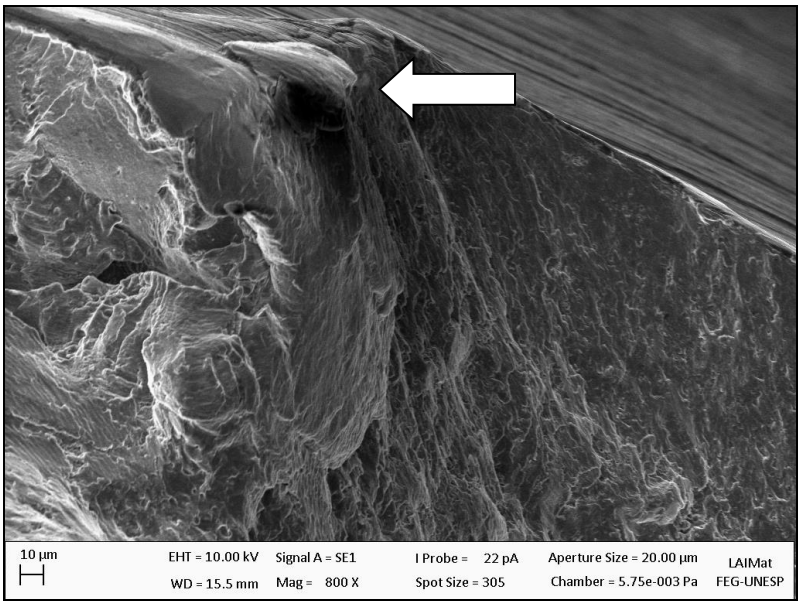

Figure 10. Fractography of the AA 6005 alloy tested at 173 MPa and fractured after 335,500 loading cycles.

ISSN 2176-5480

In Figure 11 it can be observed the fractography of a specimen of the AA 6063 alloy that broke at 107.700 cycles, at a stress amplitude of 156 MPa. It can be observed that the cracks initiation occurred at the bottom of the figure and spread up to the top, where the existence of dimples (marked area with arrow) characterizing the existence of ductile fracture is observed. When studying the fracture surfaces of the three alloys, the occurrence of ductile fracture topography of the matrix and cleavage, characteristic of brittle fracture, in the second phase particles present was observed (Figure 12. (a)). In alloys with second phase particles, it is common this ductile-fragile characteristic due the particles presents high hardness than the matrix and the fracture mechanisms act differently close these particles (ASM, 1986). The striation spacing it was observed in surface fracture of the three studied alloys (Fig. 12 (b) - AA 6063 alloy). In Figures 8-11 the striation spacing was in order of micrometers, requiring greater magnification for its observation. There were no beach tags in the surface fracture due there were no successive stops of the tests or variation in loading conditions that results in this characteristic.

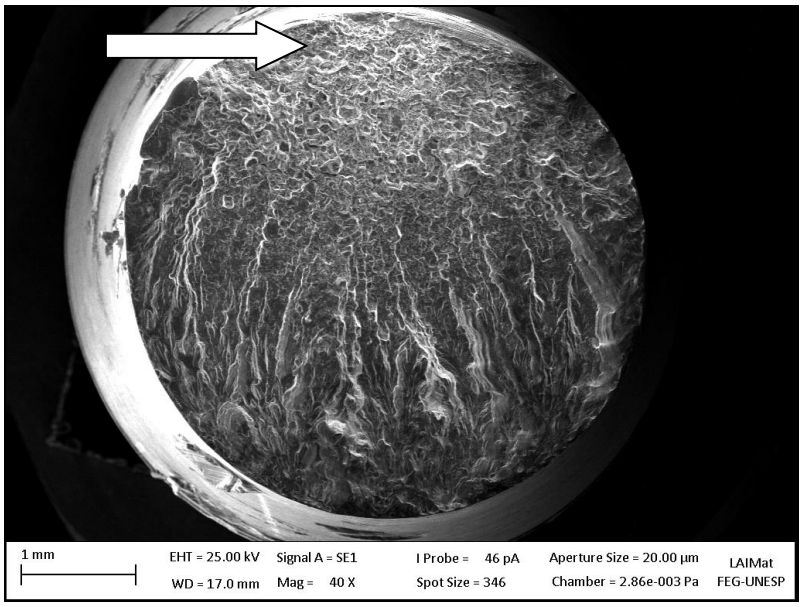

Figure 11. Fractography of the AA 6063 alloy tested at 156 MPa and fractured after 107,700 loading cycles.

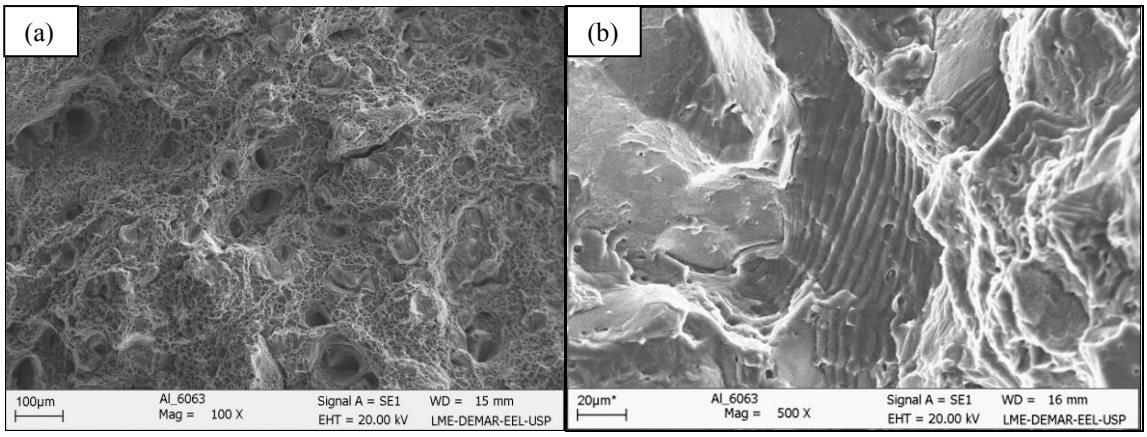

Figure 12. (a) Fractography of the AA 6063 alloy showing a surface rich of second phase particles (sample fractured in tensile test). (b) Fractography of the AA 6063 alloy tested at 177 MPa and fractured after 219,800 loading cycles.

ISSN 2176-5480

In Figure 7 (d) it can be observed the experimental points of the bending fatigue tests for three studied alloys under as-machined condition. The analysis of these points has shown that, differently from the polished condition, there is no significant difference in fatigue strength among the three alloys.

The Figure 13 (a), (b) and (c) compare the fatigue strength of the specimens under the as-machined and polished condition (Fig. 1 (a) polished/as-machined) of the studied alloys. The analysis of the figures shows that surface roughness has a clear influence on the fatigue strength of the AA 6351 alloy (Fig. 13. (c)), causing the resistance under the polished condition to be better than the resistance under the as-machined condition. However, for the alloy AA 6063 this effect was not observed (Fig. 13. (b)). There is no apparent difference among the fatigue results found under as-machined condition and polished condition in this alloy. In this figure, the curves were omitted so as to show that the points under as-machined condition are involving the points under polished condition. In addition, there is also a higher scattering of results of AA 6063 alloy when compared to AA 6351 alloy, in both cases. In AA 6063 alloy particles showed larger second phase particles (Section 3.2), which opens to speculation on whether for the AA 6063 alloy, the second phase particles have a greater effect on fatigue strength than the roughness effect. Moreover, the larger second phase particles are apparently contributing to an increasing scattering of results.

The AA 6005 alloy (Fig. 13. (a)) showed an intermediate behavior to the other two alloys. That is, there was less gain in fatigue strength for the polished condition when compared to alloy AA 6351. This effect can be explained by the higher amount of second phase particles present in this alloy (Table 3), even if the particles show a smaller size, generating a lower scattering of the fatigue results.

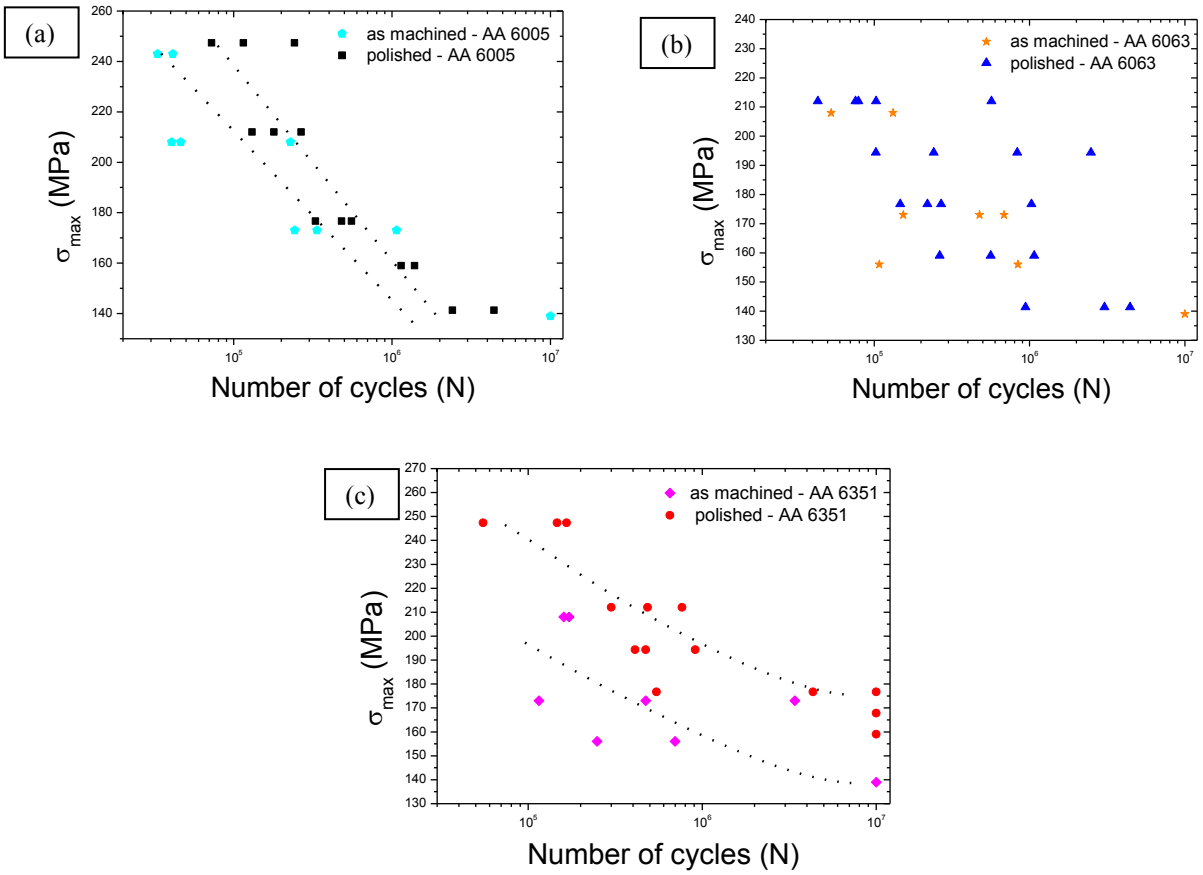

Figure 13. S/N curve of the (a) AA 6005, (b) AA 6063 and (c) AA 6351aluminum alloy (as-machined x polished).

The Figure 14 presents the results of the fatigue curves for the notched specimens (Fig. 2 (b). A better fatigue behavior of AA 6005 alloy at high cycle or low stress can be observed. In Tab. 7 it can be observed the notch sensibility calculated by the Maximum Likelihood Criterion, to 10^4 e 10^5 cycles, to three investigated alloys. The notch sensibility q and the fatigue stress concentration factor K_f were obtained by the Eq. (1) and Eq. (2) respectively:

$$q = \frac{K_f - 1}{K_t - 1} \quad (1)$$

ISSN 2176-5480

$$K_f = \frac{\sigma_{fu}}{\sigma_{fe}} \tag{2}$$

where σ_{fe} and σ_{fu} are the fatigue resistances (to a determinate fatigue life) of the notched and smooth specimens under the same experimental conditions, and K_t is the theoretical stress concentration factor, with value of 3.24 for the notched specimens used in this study (Young, 1989). The data in Tab. 7 indicate a higher notch sensitivity of the AA 6351 alloy. This effect has again shown that the AA 6351 alloy suffers greater influence of surface conditions than AA 6005 and AA 6063 alloys. The stress concentration effect in the fatigue life tends to be smaller to AA 6005 alloy in 10^5 cycles. The better notch sensibility behavior of this alloy can be related to a more difficult crack propagation, due to the higher volumetric fraction of the second phase particles present in the matrix (Tab. 3).

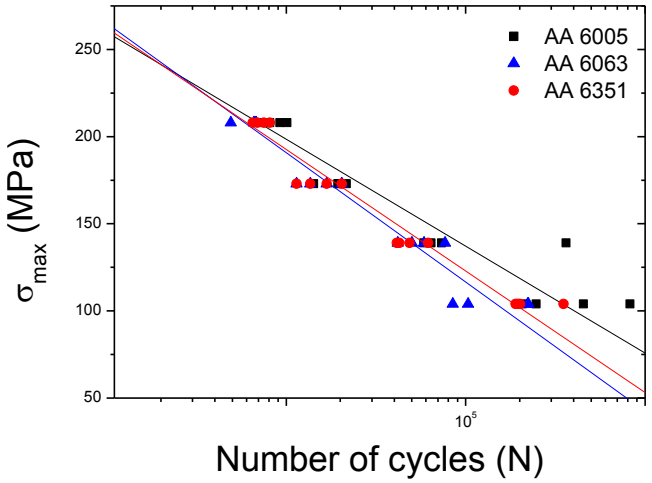

Figure 14. Model adjusting using the Maximum-Likelihood Method to AA 6005, AA 6351 and AA 6063 alloy (notched condition).

Table 7. Notch sensibility values of the AA 6005, AA 6063 and AA 6351 alloys.

AA6005		**AA6351**		**AA6063**	
Fatigue life	**q**	**Fatigue life**	**q**	**Fatigue life**	**q**
10^4	0.27	10^4	0.21	10^4	0.20
10^5	0.34	10^5	0.43	10^5	0.38

4. CONCLUSION

In this study, a comparison of the rotary bending fatigue behaviors of AA 6063, AA 6005 and AA 6351 alloys was performed under polished, as-machined and notched conditions. Under polished condition, the AA 6351 showed better fatigue behavior than the AA 6005 and AA 6063 alloys. Under as-machined condition, there were no significant differences in fatigue behavior of the three studied alloys. Therefore, AA 6351 alloy was more sensitive to variable roughness when compared to other studied alloys. On the other hand, alloy AA 6063 did not show significant difference in fatigue strength under the as-machined and polished conditions and presented a higher scattering when compared to the other two alloys. This behavior is possibly related to the larger sizes of second phase particles present in the matrix of AA 6063 alloy, which act as stress raisers and outweigh the effect of roughness. In tests with notched samples, AA 6005 alloy showed a better performance in high cycle fatigue when compared to alloys AA 6063, AA 6351. Likewise as for the roughness effect, AA 6351 alloy was also more sensitive to the presence of a notch.

5. ACKNOWLEDGEMENTS

The authors are thankful to Companhia Brasileira de Alumínio (CBA), CAPES and CNPq.

ISSN 2176-5480

6. REFERENCES

ASM International Handbook, 1986. Failure analysis and prevention. 9 th ed. Metals Park: ASM Internacional, v. 11.

ASM International Handbook, 1996. Fatigue and fracture. 9 th ed. Metals Park: ASM Internacional. v. 19.

ASTM American Society for Testing and Materials, 2010. E739-10 Standard Practice for Statistical Analysis of Linear or Linearized Stress-Life (S-N) and Strain-Life (ε-N) Fatigue Data. In: ANNUAL book of ASTM standards. Philadelphia.

Azzam, D.; Menzemer, C. C.; Srivatsan, T. S., 2010. The fracture behavior of an Al–Mg–Si alloy during cyclic fatigue, *Materials Science and Engineering*, v. A 527, p. 5341-5345.

Baptista, C. A. R. P., 2000. *Modelagem preditiva do comportamento de trincas de fadiga com aplicação ao titânio de pureza comercial*. Ph.D. thesis, Faculdade de Engenharia Química de Lorena, Lorena, Brazil.

Borrego, L. P., Costa, J. M., Silva, S., Ferreira, J. M., 2004. Microstructure dependent fatigue crack growth in aged hardened aluminum alloys. International Journal of Fatigue, v. 26, p. 1321-1331.

Burger, G. B.; Gupta, A. K.; Jeffrey, P. W.; Lloyd, D. J., 1995. Microstructural control of aluminum sheet used in automotive applications. *Mater. Charact*., v. 35, p. 23.

Cayron, C.; Buffat, P. A., 2000. Transmission electron microscopy study of the b' phase (Al-Mg-Si alloys) e QC phase (Al-Cu-Mg-Si alloys): ordening mechanism e crystallographic structure. *Acta mater*. v. 48, p. 2639-2653.

Christ, H. J., Mughrabi, H., 1996. Cyclic stress-strain response and microstructure under variable amplitude loading. Fatigue Fract Eng Mater Struct, v. 19, p. 335-348.

Espezua, S. V. P., Baptista, C. A. R. P., Nascimento, D. F. L., Silva, A. M. B., 2012. "Influence of intermetallics and precipitates on the fatigue crack nucleation and propagation in aluminum alloys 6005-T6, 6063-T6 and 6351-T6". In: *SAE Brazil Congress*, São Paulo, Brazil.

FONSECA Jr., T. M. I., 2003. *Métodos de discussão da curva-deformação vida em fadiga para as ligas de alumínio AA 6261-T6 e AA6351-T6*. Master Dissertation, Universidade Estadual de Campinas-Faculdade de Engenharia Mecânica, Campinas.

Hatch, J. E., 1984. Aluminium: Properties and physical metallurgy. Metals Park: American Society for Metals.

Laurito, D. F.; Silva, A. M. B.; Polanco, E. S. V.; Baptista, C. A. R. P., 2012. "Estudo do comportamento em fadiga de baixo ciclo das ligas de alumínio AA6005, AA6351 e AA6063". In *20º Congresso Brasileiro de Engenharia e Ciências dos Materiais-CBECIMAT*, 2012, Joinville-SC, Brazil.

Mcevily, A. J.; Endo, M.; Yamashita, K.; Ishihara, S.; Matsunaga, H., 2008. Fatigue notch sensitivity and the notch size effect. *International Journal of Fatigue*.

Polmear, I. J., 1995. Light Alloys: metallurgy of the light metals, ed. R. Honeycombe and P. Hancock. Arnold, London: *Metallurgy and Materials Science Series*.

Sadananda, K.; Ramaswamy, D. N. V., 2001. Role of crack tip plasticity in fatigue crack growth. Phylosophical Magazine A, Washington, DC, v. 81, n.5, p. 1283-1303.

Silva, A. M. B., 2012. *Estudo do comportamento em fadiga de alto ciclo e da sensibilidade ao entalhe das ligas de alumínio AA 6005 T6, AA 6063 T6 e AA 6351 T6***.** 145 f. Master dissertation, Universidade de São Paulo - EEL/USP, Lorena, Brazil.

Silva, A. M. B.; Laurito, D. F.; Polanco, E. S. V.; Baptista, C. A. R. P. ; Torres, M. A. S., 2012. "Estudo do comportamento em fadiga de alto ciclo e da sensibilidade ao entalhe das ligas de alumínio AA6005 T6, AA6351 T6 e AA 6063 T6". In *20º Congresso Brasileiro de Engenharia e Ciências dos Materiais-CBECIMAT*, Joinville-SC, Brazil.

Suresh, S., 1998. Fatigue of materials. 2th ed. New York: Cambridge University Press.

Young, W. C., 1989. Roark's formulas for stress and strain. 6th ed. New York:McGraw-Hill.

7. RESPONSIBILITY NOTICE

The authors are the only responsible for the printed material included in this paper.